

New Members of the $\{\text{Fe}(\text{NO})_2\}^{10}$ Dinitrosyliron Complexes Bound with [Thiolate, Thiolate] and [Amide, Amide] Ligations

Jheng-Hong Wang[†] and Chien-Hong Chen^{*,†,‡}

[†]School of Applied Chemistry, Chung Shan Medical University, Taichung City 40201, Taiwan, and

[‡]Department of Medical Research, Chung Shan Medical University Hospital, Taichung City, Taiwan

Received June 3, 2010

The first dianionic $\{\text{Fe}(\text{NO})_2\}^{10}$ dinitrosyliron complexes (DNICs) $[\text{Fe}(\text{SC}_7\text{H}_4\text{SN})_2(\text{NO})_2]^{2-}$ (**1**) and $[\text{Fe}(\text{OC}_7\text{H}_4\text{SN})_2(\text{NO})_2]^{2-}$ (**2**), coordinated with thiolates and amides, were prepared by the reaction of $\text{Fe}(\text{TMEDA})(\text{NO})_2$ with 2 equiv of ligands $[\text{SC}_7\text{H}_4\text{SN}]^-$ and $[\text{OC}_7\text{H}_4\text{SN}]^-$, respectively. The reversible interconversion between the dianionic $\{\text{Fe}(\text{NO})_2\}^{10}$ DNICs **1/2** and the anionic $\{\text{Fe}(\text{NO})_2\}^9[\text{Fe}(\text{SC}_7\text{H}_4\text{SN})_2(\text{NO})_2]^-$ (**3**)/ $[\text{Fe}(\text{OC}_7\text{H}_4\text{SN})_2(\text{NO})_2]^-$ (**4**), respectively, was demonstrated. The transformation of DNICs **2** and **3** into the thermally stable DNICs **1** and **4**, respectively, via the ligand-exchange reaction reveals that $[\text{OC}_7\text{H}_4\text{SN}]^-$ shows a high binding affinity toward the $\{\text{Fe}(\text{NO})_2\}^9$ motif and $[\text{SC}_7\text{H}_4\text{SN}]^-$ prefers the $\{\text{Fe}(\text{NO})_2\}^{10}$ motif. This result rationalizes that the intermolecular electron transfer from DNIC **2** to DNIC **3** occurs to lead to the formation of the more thermally stable DNICs **1** and **4** upon the reaction of DNICs **2** and **3** in tetrahydrofuran.

Interest in nitric oxide (NO) derives from its physiological and biological functions in living organisms.¹ In vivo, NO can be stabilized and stored in the two forms protein-bound thionitrosyls ($\text{R}_{\text{protein}}\text{SNO}$) and protein-bound dinitrosyliron complexes (protein-bound DNICs).² The displacement of protein-bound DNICs with free thiols/thiolates yielding low-molecular-weight DNICs (LMW-DNICs) has been suggested.³ In vitro/in vivo, both protein-bound DNICs and LMW-DNICs are possibly identified and characterized by their distinctive electron paramagnetic resonance (EPR) signals at

$g = 2.03$.⁴ In spite of the major thiol components of cellular DNICs composed of cysteine and glutathione in vivo,⁵ DNICs ligated by phenoxide, thiolate, imidazole, and deprotonated imidazole were proposed in enzymology based on EPR spectra.^{3a,6} Recently, the protein-bound DNIC with [S, O] ligation has been well characterized by an X-ray diffraction study via the addition of a dinitrosyldiglutathionyliron complex into human glutathione transferase P1-1 in vitro/in vivo.^{6c} In biomimetic complexes, varieties of DNICs containing S/O/N-donor ligands were synthesized to serve as spectroscopic references.^{7,8} On the basis of the Enemark–Fetham

(4) (a) Butler, A. R.; Megson, I. L. *Chem. Rev.* **2002**, *102*, 1155–1165. (b) Cooper, C. E. *Biochim. Biophys. Acta, Bioenergy* **1999**, *1411*, 290–309. (c) Foster, M. W.; Cowan, J. A. *J. Am. Chem. Soc.* **1999**, *121*, 4093–4100. (d) Vithayathil, A. J.; Ternberg, J. L.; Commoner, B. *Nature* **1965**, *207*, 1246–1249.

(5) Lewandowska, H.; Meczynska, S.; Sochanowicz, B.; Sadlo, J.; Kruszewski, M. *J. Biol. Inorg. Chem.* **2007**, *12*, 345–352.

(6) (a) Ding, H.; Demple, B. *Proc. Natl. Acad. Sci. U.S.A.* **2000**, *97*, 5146–5150. (b) Turella, P.; Pedersen, J. Z.; Caccuri, A. M.; De Maria, F.; Mastroberardino, P.; Lo Bello, M.; Federici, G.; Ricci, G. *J. Biol. Chem.* **2003**, *278*, 42294–42299. (c) Cesareo, E.; Parker, L. J.; Pedersen, J. Z.; Nuccetelli, M.; Mazzetti, A. P.; Pastore, A.; Federici, G.; Caccuri, A. M.; Ricci, G.; Adams, J. J.; Parker, M. W.; Lo Bello, M. *J. Biol. Chem.* **2005**, *280*, 42172–42180. (d) D'Autreux, B.; Horner, O.; Oddou, J.-L.; Jeandey, C.; Gambarelli, S.; Berthomieu, C.; Latour, J.-M.; Michaud-Soret, I. *J. Am. Chem. Soc.* **2004**, *126*, 6005–6016.

(7) (a) Tsai, M.-L.; Chen, C.-C.; Hsu, I. J.; Ke, S.-C.; Hsieh, C.-H.; Chiang, K.-A.; Lee, G.-H.; Wang, Y.; Chen, J.-M.; Lee, J.-F.; Liaw, W.-F. *Inorg. Chem.* **2004**, *43*, 5159–5167. (b) Tsai, F. T.; Chiou, S. J.; Tsai, M. C.; Tsai, M. L.; Huang, H. W.; Chiang, M. H.; Liaw, W. F. *Inorg. Chem.* **2005**, *44*, 5872–5881. (c) Lu, T.-T.; Chiou, S.-J.; Chen, C.-Y.; Liaw, W.-F. *Inorg. Chem.* **2006**, *45*, 8799–8806. (d) Tsai, M.-L.; Liaw, W.-F. *Inorg. Chem.* **2006**, *45*, 6583–6585. (e) Hung, M.-C.; Tsai, M.-C.; Lee, G.-H.; Liaw, W.-F. *Inorg. Chem.* **2006**, *45*, 6041–6047. (f) Tsai, M. L.; Hsieh, C. H.; Liaw, W. F. *Inorg. Chem.* **2007**, *46*, 5110–5117. (g) Huang, H.-W.; Tsou, C.-C.; Kuo, T.-S.; Liaw, W.-F. *Inorg. Chem.* **2008**, *47*, 2196–2204. (h) Chiou, S.-J.; Wang, C.-C.; Chang, C.-M. *J. Organomet. Chem.* **2008**, *693*, 3582–3586. (i) Wang, X.; Sundberg, E. B.; Li, L.; Kantardjeff, K. A.; Herron, S. R.; Lim, M.; Ford, P. C. *Chem. Commun.* **2005**, 477–479. (j) Tsai, M.-C.; Tsai, F.-T.; Lu, T.-T.; Tsai, M.-L.; Wei, Y.-C.; Hsu, I.-J.; Lee, J.-F.; Liaw, W.-F. *Inorg. Chem.* **2009**, *48*, 9579–9591.

(8) (a) Reginato, N.; McCrory, C. T. C.; Pervitsky, D.; Li, L. *J. Am. Chem. Soc.* **1999**, *121*, 10217–10218. (b) Wang, R.; Wang, X.; Sundberg, E. B.; Nguyen, P.; Grant, G. P.; Sheth, C.; Zhao, Q.; Herron, S.; Kantardjeff, K. A.; Li, L. *Inorg. Chem.* **2009**, *48*, 9779–9785. (c) Albano, V. G.; Araneo, A.; Bellon, P. L.; Ciani, G.; Manassero, M. *J. Organomet. Chem.* **1974**, *67*, 413–422. (d) Atkinson, F. L.; Blackwell, H. E.; Brown, N. C.; Connelly, N. G.; Crossley, J. G.; Orpen, A. G.; Rieger, A. L.; Rieger, P. H. *Dalton Trans.* **1996**, 3491–3502. (e) Tonzetich, Z. J.; Do, L. H.; Lippard, S. J. *J. Am. Chem. Soc.* **2009**, *131*, 7964–7965.

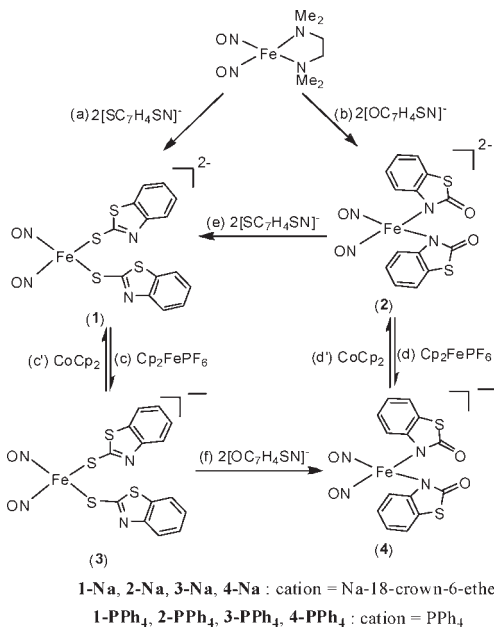
*To whom correspondence should be addressed. E-mail: cchwind@csmu.edu.tw.

(1) (a) Jaimes, E. A.; del Castillo, D.; Rutherford, M. S.; Raji, L. *J. Am. Soc. Nephrol.* **2001**, *12*, 1204–1210. (b) May, G. C. P.; Moore, P. K.; Page, C. P. *Br. J. Pharmacol.* **1991**, *102*, 759–763. (c) Tao, Y. P.; Misko, T. P.; Howlette, A. C.; Klein, C. *Development* **1997**, *124*, 3587–3595. (d) MacMicking, J.; Xie, Q.; Nathan, C. *Annu. Rev. Immunol.* **1997**, *15*, 323–350.

(2) (a) McCleverty, J. A. *Chem. Rev.* **2004**, *104*, 403–418. (b) Badorff, C.; Fichtlscherer, B.; Muelsch, A.; Zeiher, A. M.; Dimmeler, S. *Nitric Oxide* **2002**, *6*, 305–312. (c) Stamler, J. S.; Singel, D. J.; Loscalzo, J. *Science* **1992**, *258*, 1898–1902. (d) Stamler, J. S. *Cell* **1994**, *78*, 931–936.

(3) (a) Boese, M.; Mordvintcev, P. I.; Vanin, A. F.; Busse, R.; Muelsch, A. *J. Biol. Chem.* **1995**, *270*, 29244–29249. (b) Henry, Y.; Lepoitvre, M.; Drapier, J. C.; Ducrocq, C.; Boucher, J. L.; Guissani, A. *FASEB J.* **1993**, *7*, 1124–1134. (c) Radi, R.; Beckman, J. S.; Bush, K. M.; Freeman, B. A. *J. Biol. Chem.* **1991**, *266*, 4244–4250. (d) Muelsch, A. *Drug Res.* **1994**, *44*, 408–411. (e) Vanin, A. F.; Mordvintcev, P. I.; Hauschildt, S.; Muelsch, A. *Biochim. Biophys. Acta, Mol. Cell Res.* **1993**, *1177*, 37–42.

Scheme 1



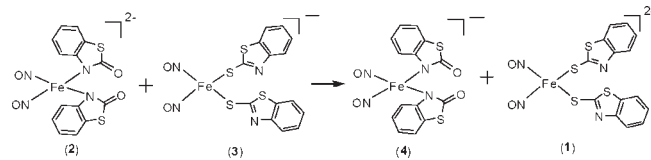
notation,⁹ these synthesized LMW-DNICs can be classified as the EPR-active $\{\text{Fe}(\text{NO})_2\}^9$ DNICs and the EPR-silent $\{\text{Fe}(\text{NO})_2\}^{10}$ DNICs. In spite of a large number of neutral $\{\text{Fe}(\text{NO})_2\}^{10}$ DNICs with nitrogen or phosphorus ligands, the dianionic $\{\text{Fe}(\text{NO})_2\}^{10}$ DNICs are limited.⁸ Recently, we report the monoanionic sulfur-containing $\{\text{Fe}(\text{NO})_2\}^{10}$ DNIC [K-18-crown-6-ether][Fe(SC₆H₄-*o*-NMe₂)(NO)₂].¹⁰ In addition to the classical four-coordinate DNICs, the nonclassical DNICs, including the five-coordinate DNICs [(6-Me₃-TPA)Fe(NO)₂]⁺ and [(TMEDA)Fe(NO)₂I],^{11,12} and the six-coordinate DNIC[(1-Melm)₂(η^2 -ONO)Fe(NO)₂]¹³ are also structurally characterized. In this contribution, the dianionic $\{\text{Fe}(\text{NO})_2\}^{10}$ DNICs with [thiolate, thiolate] and [amide, amide] ligation, [Fe(SC₇H₄SN)₂(NO)₂]²⁻ (**1**) and [Fe(OC₇H₄SN)₂(NO)₂]²⁻ (**2**) [cation = Na-18-crown-6-ether (**1-Na**/**2-Na**), PPh₄ (**1-PPh₄**/**2-PPh₄**)], were delineated. The reversible interconversion among the dianionic $\{\text{Fe}(\text{NO})_2\}^{10}$ DNICs **1/2** and the anionic $\{\text{Fe}(\text{NO})_2\}^9$ DNICs [Fe(SC₇H₄SN)₂(NO)₂]⁻ (**3**)/[Fe(OC₇H₄SN)₂(NO)₂]⁻ (**4**) [cation = Na-18-crown-6-ether (**3-Na**/**4-Na**), PPh₄⁺ (**3-PPh₄**/**4-PPh₄**)] was demonstrated. In particular, the different binding affinities of [OC₇H₄SN]⁻ versus [SC₇H₄SN]⁻ toward the $\{\text{Fe}(\text{NO})_2\}^9/\{\text{Fe}(\text{NO})_2\}^{10}$ motif were studied.

The reaction of Fe(TMEDA)(NO)₂ with 2 equiv of [SC₇H₄SN]⁻ and [OC₇H₄SN]⁻ yielded DNICs **1** and **2** characterized by single-crystal X-ray diffraction, IR, and UV-vis spectra, respectively (Scheme 1a,b). DNICs **1** and **2** display the EPR-silent $\{\text{Fe}(\text{NO})_2\}^{10}$ electronic structures with [thiolate, thiolate]/[amide, amide] ligation mode. Compared to the other $\{\text{Fe}(\text{NO})_2\}^{10}$ DNICs, **1-PPh₄** is the first example of the dianionic mononuclear $\{\text{Fe}(\text{NO})_2\}^{10}$ DNICs coordinated with two thiolate ligands.

(9) Enemark, J. H.; Feltham, R. D. *Coord. Chem. Rev.* **1974**, *13*, 339–406.
 (10) Chen, C. H.; Chiou, S. J.; Chen, H. Y. *Inorg. Chem.* **2010**, *49*, 2023–2025.

(11) Jo, D.-H.; Chiou, Y.-M.; Que, L., Jr. *Inorg. Chem.* **2001**, *40*, 3181–3190.
 (12) Chen, C.-H.; Ho, Y.-C.; Lee, G.-H. *J. Organomet. Chem.* **2009**, *694*, 3395–3400.
 (13) Tsai, F. T.; Kuo, T. S.; Liaw, W. F. *J. Am. Chem. Soc.* **2009**, *131*, 3426–3427.

Scheme 2



Upon the addition of Cp₂FePF₆ into the CH₃CN solution of DNICs **1** and **2** in a 1:1 stoichiometry, respectively (Scheme 1c,d), oxidation ensued over the course of 5 h to yield the $\{\text{Fe}(\text{NO})_2\}^9$ DNICs **3** and **4**, respectively, identified by EPR and IR spectra. In contrast to ligand-centered oxidation of the thiolate-containing $\{\text{Fe}(\text{NO})_2\}^9$ DNICs resulting in dimeric $\{\text{Fe}(\text{NO})_2\}^9-\{\text{Fe}(\text{NO})_2\}^9$ Roussin's red esters (RREs),^{7c,f} the isolation of DNIC **3** may reveal that oxidation of the thiolate-containing $\{\text{Fe}(\text{NO})_2\}^{10}$ DNICs is a metal-centered process.

In cyclic voltammograms of **3-PPh₄** and **4-PPh₄**, the quasi-reversible one-electron reductions at -0.94 and -1.17 V ($E_{1/2}$ vs Fc⁺/Fc), respectively, in CH₃CN are observed and assigned to the $\{\text{Fe}(\text{NO})_2\}^9-\{\text{Fe}(\text{NO})_2\}^{10}$ couple (Figure S1 in the Supporting Information). The slightly negative reduction potential of **4-PPh₄** versus that of **3-PPh₄** indicates that [OC₇H₄SN]⁻ has a stronger electron-donating ability than [SC₇H₄SN]⁻. The chemical reduction of **3-PPh₄** and **4-PPh₄** with CoCp₂ (Scheme 1c',d') afforded $\{[\text{PPh}_4][\text{CoCp}_2]\}\{\text{[Fe}(\text{SC}_7\text{H}_4\text{SN})_2(\text{NO})_2]\}$ and $\{[\text{PPh}_4][\text{CoCp}_2]\}\{\text{[Fe}(\text{OC}_7\text{H}_4\text{SN})_2(\text{NO})_2]\}$, respectively, characterized by Fourier transform IR. The reduction process is also consistent with the $\{\text{Fe}(\text{NO})_2\}^9-\{\text{Fe}(\text{NO})_2\}^{10}$ couple in the cyclic voltammogram of **3-PPh₄**/**4-PPh₄**. In contrast to the reduction of the thiolate-containing $\{\text{Fe}(\text{NO})_2\}^9$ DNICs leading to the dissociation of thiolate of DNICs reported previously,^{7b} the redox reaction of DNICs **3** and **1** displays the reversible interconversion between the thiolate-containing $\{\text{Fe}(\text{NO})_2\}^9$ and $\{\text{Fe}(\text{NO})_2\}^{10}$ DNICs.

The relative affinity of the different ligands toward the $\{\text{Fe}(\text{NO})_2\}^9$ motif has been studied by Liaw et al. via the ligand-exchange experiments.^{7b,g,j} Similarly, the coordinated ligands [SC₇H₄SN]⁻ of $\{\text{Fe}(\text{NO})_2\}^9$ **3-PPh₄** could be replaced by the stronger donor [OC₇H₄SN]⁻ to yield the more stable **4-PPh₄** (Scheme 1f). Interestingly, the addition of 2 equiv of [SC₇H₄SN]⁻ to the tetrahydrofuran (THF) solution of $\{\text{Fe}(\text{NO})_2\}^{10}$ **2-Na** led to the light-green precipitates of the more stable **1-Na**, characterized by IR spectra (Scheme 1e). The different binding affinities of [OC₇H₄SN]⁻ and [SC₇H₄SN]⁻ toward the $\{\text{Fe}(\text{NO})_2\}$ core of DNICs reveal that the electron-rich $\{\text{Fe}(\text{NO})_2\}^{10}$ motif prefers the binding of the less electron-donating ligand [SC₇H₄SN]⁻. In contrast, the stronger electron-donating ligand [OC₇H₄SN]⁻ favors coordination to the electron-deficient $\{\text{Fe}(\text{NO})_2\}^9$ motif. This rationalization may support the fact that the reaction of $\{\text{Fe}(\text{NO})_2\}^{10}$ **2-PPh₄** and $\{\text{Fe}(\text{NO})_2\}^9$ **3-PPh₄** afforded the relatively stable $\{\text{Fe}(\text{NO})_2\}^9$ **4-PPh₄** and $\{\text{Fe}(\text{NO})_2\}^{10}$ **1-PPh₄** via intermolecular electron transfer in THF (Scheme 2).

Figures 1 and 2 display the thermal ellipsoid plots of the dianionic **1-PPh₄** and **2-PPh₄**, respectively, and the selected bond angles and bond lengths are given in the figure captions, respectively. The structures of **1-PPh₄** and **2-PPh₄** contain a four-coordinate iron center in a distorted tetrahedral geometry. Comparisons of the mean Fe–S bond distances [2.2941(18) Å in [PPN][Fe(SC₇H₄SN)₂(NO)₂]⁻^{7b} vs 2.3460(13) Å in **1-PPh₄**] and Fe–N bond distances [1.993(2) Å in **4-PPh₄** (Figure S2 in the Supporting Information) vs 2.094(2) Å in **2-PPh₄**] reveal

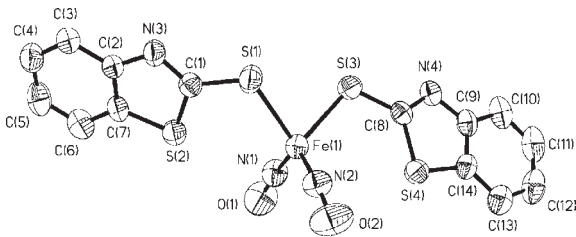


Figure 1. Structure of the anion of **1-PPh₄** displaying 50% thermal ellipsoids for all non-hydrogen atoms. Selected bond distances (\AA) and angles (deg): Fe(1)–N(1), 1.645(4); Fe(1)–N(2), 1.642(4); Fe(1)–S(1), 2.3679(13); Fe(1)–S(3), 2.3240(13); N(1)–O(1), 1.193(4); N(2)–O(2), 1.205(4); Fe(1)–N(1)–O(1), 168.3(4); Fe(1)–N(2)–O(2), 167.6(4); N(1)–Fe(1)–N(2), 115.34(19); S(1)–Fe(1)–S(3), 84.48(5).

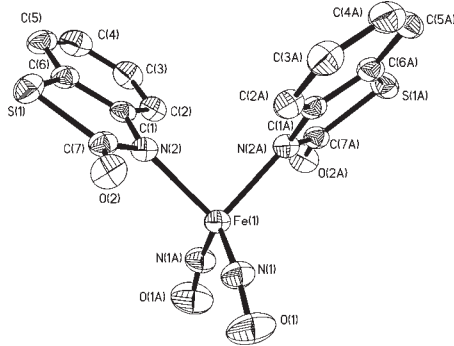


Figure 2. Structure of the anion of **2-PPh₄** displaying 50% thermal ellipsoids for all non-hydrogen atoms. Selected bond distances (\AA) and angles (deg): Fe(1)–N(1), 1.638(3); Fe(1)–N(2), 2.094(2); N(1)–O(1), 1.203(3); N(1)–Fe(1)–N(1A), 110.45(19); N(2)–Fe(1)–N(2A), 88.80(13); Fe(1)–N(1)–O(1), 164.6(3).

that reduction of the $\{\text{Fe}(\text{NO})_2\}^9$ core to the $\{\text{Fe}(\text{NO})_2\}^{10}$ core leads to elongation of the Fe–N and Fe–S distances. Meanwhile, the shorter Fe–N(O) bond distances of 1.644(4) and 1.638(3) \AA and the longer N–O bond distances of 1.199(4) and 1.203(3) \AA found in **1-PPh₄** and **2-PPh₄**, respectively, compared to the Fe–N(O) bond distances of 1.684(6) and 1.687(2) \AA and the N–O bond distances of 1.174(6) and 1.175(3) \AA found in $[\text{PPN}][\text{Fe}(\text{SC}_7\text{H}_4\text{SN})_2(\text{NO})_2]$ and **4-PPh₄**, respectively, are consistent with a relatively considerable degree of π -back-bonding in the $\{\text{Fe}(\text{NO})_2\}^{10}$ core. In contrast to the distinct bond distances in $[\text{PPN}][\text{Fe}(\text{SC}_7\text{H}_4\text{SN})_2(\text{NO})_2]$ and **1-PPh₄/4-PPh₄** and **2-PPh₄**, the comparable Fe–N–O bond angles [169.9(5) $^\circ$ in $[\text{PPN}][\text{Fe}(\text{SC}_7\text{H}_4\text{SN})_2(\text{NO})_2]$] vs 168.0(4) $^\circ$ in **1-PPh₄** and 163.6(2) $^\circ$ in **4-PPh₄** vs 164.6(3) $^\circ$ in **2-PPh₄**] are observed when the $\{\text{Fe}(\text{NO})_2\}^9$ DNICs are reduced to the structurally analogous $\{\text{Fe}(\text{NO})_2\}^{10}$ DNICs.

($\text{SC}_7\text{H}_4\text{SN})_2(\text{NO})_2$] vs 168.0(4) $^\circ$ in **1-PPh₄** and 163.6(2) $^\circ$ in **4-PPh₄** vs 164.6(3) $^\circ$ in **2-PPh₄**] are observed when the $\{\text{Fe}(\text{NO})_2\}^9$ DNICs are reduced to the structurally analogous $\{\text{Fe}(\text{NO})_2\}^{10}$ DNICs.

In summary, the dianionic $\{\text{Fe}(\text{NO})_2\}^{10}$ DNICs containing [thiolate, thiolate]/[amide, amide] ligation were isolated and structurally characterized. The synthetic methodology reveals that $\text{Fe}(\text{TMEDA})(\text{NO})_2$ acts as an $\{\text{Fe}(\text{NO})_2\}^{10}$ motif donor reagent in the presence of thiolates and amides. The redox reaction between DNICs **1/2** and **3/4** successfully demonstrates the reversible interconversion with no dissociation of the coordinated ligands of the structurally analogous $\{\text{Fe}(\text{NO})_2\}^9/\{\text{Fe}(\text{NO})_2\}^{10}$ DNICs. The ligand substitution reactions of DNICs **2** and **3** to form the relatively stable DNICs **1** and **4**, respectively, have demonstrated that the $\{\text{Fe}(\text{NO})_2\}^9$ motif shows a strong preference for the stronger electron-donating ligands over the weaker electron-donating ligands; however, the $\{\text{Fe}(\text{NO})_2\}^{10}$ motif shows a stronger binding affinity toward the weaker electron-donating ligands. In addition to the ligand-exchange reactions yielding the more stable DNICs,^{7b,g,j} the reaction of $\{\text{Fe}(\text{NO})_2\}^{10}$ **2-PPh₄** and $\{\text{Fe}(\text{NO})_2\}^9$ **3-PPh₄** yielding the relatively stable $\{\text{Fe}(\text{NO})_2\}^9$ **4-PPh₄** and $\{\text{Fe}(\text{NO})_2\}^{10}$ **1-PPh₄** may signify that the intermolecular electron transfer between $\{\text{Fe}(\text{NO})_2\}^{10}$ and $\{\text{Fe}(\text{NO})_2\}^9$ DNICs is the alternative mechanism to afford the more stable DNICs for transport and storage of NO in biology. Studies on the electronic structure (NO/Fe oxidation states) of the series of $\{\text{Fe}(\text{NO})_2\}^9/\{\text{Fe}(\text{NO})_2\}^{10}$ DNICs by X-ray absorption spectroscopy and density functional theory calculations are ongoing. Also, the binding preference of a series of ligands toward $\{\text{Fe}(\text{NO})_2\}^9/\{\text{Fe}(\text{NO})_2\}^{10}$ motifs is currently being investigated in our laboratory.

Acknowledgment. We gratefully acknowledge financial support from the National Science Council of Taiwan. The authors thank Professor Liaw for valuable discussions and Gene-Hsiang Lee and Ting-Shen Kuo for the single-crystal X-ray structural determinations.

Supporting Information Available: X-ray crystallographic files in CIF format for the structural determinations of complexes **1-PPh₄**, **2-PPh₄**, and **4-PPh₄**, experimental details, crystallographic data and refinement parameters, and bond distances and angles. This material is available free of charge via the Internet at <http://pubs.acs.org>.